13th World Conference on Earthquake Engineering
Vancouver, B.C., Canada
August 1-6, 2004
Paper No. 503

BUCKLING RESTRAINED BRACES FOR DUCTILE END CROSS FRAMES IN STEEL PLATE GIRDER BRIDGES

Lyle CARDEN[1], Ahmad ITANI[2], Ian BUCKLE[3] and Ian AIKEN[4]

SUMMARY

Buckling restrained braces (BRBs) have been shown to be effective in the seismic design of buildings. In this project BRBs were investigated as ductile end cross frames in steel plate girder bridges. Component experiments on a series of braces showed that they exhibited good cyclic behavior although loading history and strain rate affected the performance of these braces. Unbonded braces used as ductile end cross frames were able to reduce the shear demand in a bridge model more effectively than angle X-braces during shake table experiments. Ductile end cross frames are believed to be most effective when both the superstructure and substructure are relatively rigid.

INTRODUCTION

The end cross frames or diaphragms in steel plate girder bridges have been determined to be critical in the transverse load path for seismic loading. Past earthquakes have resulted in damage to these end cross frames as described by Astaneh-Asl [1], Bruneau [2] and Shinozuka [3]. It has become apparent that the end cross frames need to be designed for the transverse earthquake loading [4]. There are essentially two approaches which can be considered in their design. The first is to design them to perform elastically, protected by the capacity design of the substructure as described by Itani [5]. The second is to design the cross frames to be ductile and use these ductile elements to protect other parts of the superstructure and substructure. Studies have been performed by Astaneh-Asl [6] and Zahrai [7, 8] investigating the potential for use of cross frames as ductile elements. These studies investigated different systems, including special cross braces, shear panel systems (SPS), eccentric braced frames (EBF) and a triangular-plate added damping and stiffness (TADAS) device. The studies demonstrated the feasibility of ductile end cross frames as long as the substructure is not too flexible.

Buckling restrained braces (BRBs) have emerged as an attractive form of bracing in buildings during earthquakes. They have been shown to have good hysteretic behavior without stiffness and strength degradation as observed in concentric braced framing systems. In this project buckling restrained braces were investigated as a potential form of ductile end cross frame in steel plate girder bridges. For this

[1] Graduate Assistant, University of Nevada, Reno, NV, U.S.A., Email: lcarden@unr.edu
[2] Associate Professor, University of Nevada, Reno, NV, U.S.A., Email: itani@unr.edu
[3] Professor, University of Nevada, Reno, NV, U.S.A., Email: igbuckle@unr.edu
[4] Seismic Isolation Engineering, Oakland, CA, U.S.A., Email: ida@siecorp.com

application the braces were shorter in length compared to those typically used in buildings, making the connection details particularly important. They also had a relatively small core dimensions.

In order to perform experiments on ductile end cross frames with buckling restrained braces, a $^2/_5{}^{th}$ scale model of a two steel plate girder bridge superstructure was used, as shown in Figure 1. "Unbonded" braces, a type of BRB constructed by Nippon Steel Corporation using low yield point (LYP-225) steel, were placed diagonally at the ends of the bridge model as shown. The end cross frames also consisted of a top chord to provide a direct load path for transverse earthquake loads between the deck and the end cross frames, with implications as described by Carden [9]. A bottom chord was also provided to evenly distribute loads between the bearings. The top and bottom chords were constructed with pinned connections to minimize their lateral stiffness and therefore minimize post-yield stiffness in the ductile end cross frames. Several shear studs connecting the deck and the girders were removed at the ends of the girders in order to allow the girders to rotate about their longitudinal axis to further minimize post-yield stiffness in the ductile end cross frames. Transverse earthquake loading was simulated using shake tables at either end of the bridge model. Experiments were also performed on the bridge model with special angle X-braces and with seismic isolation bearings although the results from these experiments are referred to only briefly in this paper.

COUPON TESTS

Two coupon tests were performed by Nippon Steel [10] on the LYP-225 steel used in the unbonded braces. The resulting material properties for the two tests are given in Table 1. The yield strength of the steel coupons was shown to be close to the expected yield strength of 225 MPa. Unlike most US steels where the nominal strength is generally defined at a minimum specified strength, the nominal strength for the LYP-225 steel is defined in the middle of a relatively tight range of acceptable yield strengths. Therefore, the nominal strength of 225 ksi was taken as the expected strength for this material. The ultimate strength of the LYP-225 steel was around 30% higher than the yield strength, compared to 50% for comparable A36 steel coupons tested for this project, indicating less strain hardening in LYP-225 steel. The ultimate strain was much higher at around 65% for the LYP-225 steel compared to 30-35% for the A36 steel.

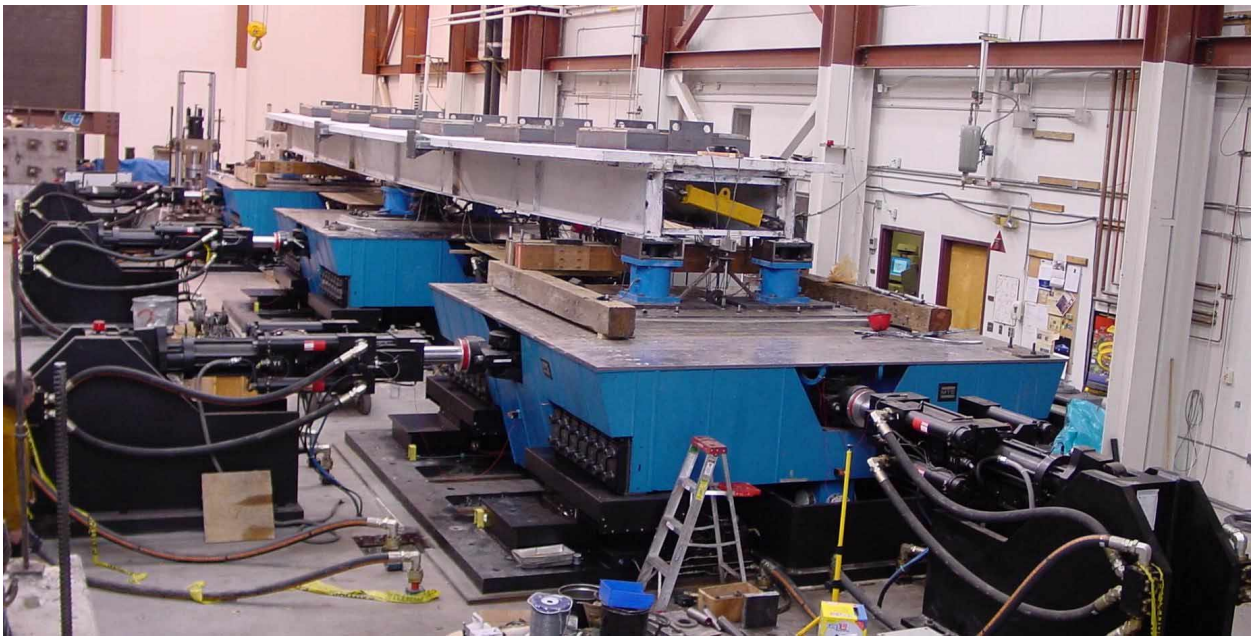

Figure 1. Shake Table Experiment on Bridge Model with Unbonded Braces

Table 1: Properties of LYP-225 Steel from Coupon Tests

Coupon Test #		#1	#2
Yield Stress	(MPa)	223	235
Ultimate Stress	(MPa)	302	302
Ultimate Elongation	(%)	64	65

AXIAL COMPONENT EXPERIMENTS

Overview

Component experiments were performed on unbonded braces identical to those used in the bridge model in order to characterize the properties of the braces and compare these to the design properties. Of seven braces provided, four were used solely for component experiments, and the remaining three were used in bridge experiments before being tested to failure in the component experiment assembly. Axial component experiments were performed to evaluate overall brace behavior, cumulative displacement capacity of the braces, the effect of different loading histories, and the effect of dynamic loading.

Experimental Setup and Loading

Axial loads were applied to the unbonded braces using an MTS load frame as shown in Figure 2. The overall length of the brace was equal to 968 mm (38 $^{1}/_{8}$ in). The deformable length was calculated to be 518 mm (20 $^{3}/_{8}$ in) between the centres of the transitions from the maximum cruciform to the minimum core sections. The core plate was equal to 25 x 16 mm (1 x $^{5}/_{8}$ in). The first brace was connected to grip plates in the load frame with pin ended connections. This connection was designed to be an ideal pin for rotation in the plane of the cross frame. Out of plane partial fixity was provided using gusset plates on either side of the bearing stiffener as illustrated in Figure 2a. The remaining braces were tested with fixed connections which were designed to be slip-critical based on the serviceability criteria in the AISC LRFD provisions [11].

Three of the unbonded braces were instrumented with four strain gauges to measure strains on each side of the plate at each end of the deformable length. The braces were also instrumented with two displacement transducers on either side of the brace to measure displacements across the deformable length, as shown in Figure 2. The displacement was also measured at the head of the actuator to give the total displacement including deformations in the connection regions. The axial force was measured by the actuator load cell.

The loading history for each of the braces differed. Unbonded Brace A was subjected to a modified ATC-24 [12] loading history. This history subjected the brace to two cycles at each excursion and was based on the expected force up until yielding then continued based on the displacement at yield. As slippage in the pinned connection was considerable, the history was modified to achieve reasonable displacements in the deformable region. The loading rate for this history was slow.

The loading history for the second brace (Brace B) was based on the loading history in the draft Recommended Provisions for Buckling-Restrained Brace Frames (BRBF) by SEAONC [13]. The loading history is defined by a number of cycles at different levels of displacement ductility. After applying the prescribed cycles of increasing amplitudes each specimen was cycled at a constant amplitude until failure at the maximum displacement amplitude. The displacements were controlled using the total displacements measured in the actuator. The yield displacement used to define the loading history was based on the estimated displacement calculated at a 0.2% offset strain which was equal to 1.63 mm (0.064

in). No slippage was observed before yielding therefore it did not affect the yield displacement. It is important to note that the displacement at 0.2% offset strain was considerably higher than the yield displacement if estimated using the ATC-24 procedure based on the slope at 75% of the yield force. As the BRBF guidelines do not define the way in which the yield displacement is to be estimated, the 0.2% strain method which resulted in the more severe displacements was used. The loading history for Unbonded Brace C was the reverse of the BRBF loading history, and therefore had the maximum amplitude cycles at the beginning of the history, followed by smaller cycles. At the end of the history the brace was subjected to the maximum amplitude cycles to failure. The loading history for Unbonded Brace C was applied at a slow rate. For Unbonded Brace D the same loading history as for Brace C was used, but this time applied dynamically to the brace at a frequency of 2 Hz, to simulate a bridge with a 0.5s effective period.

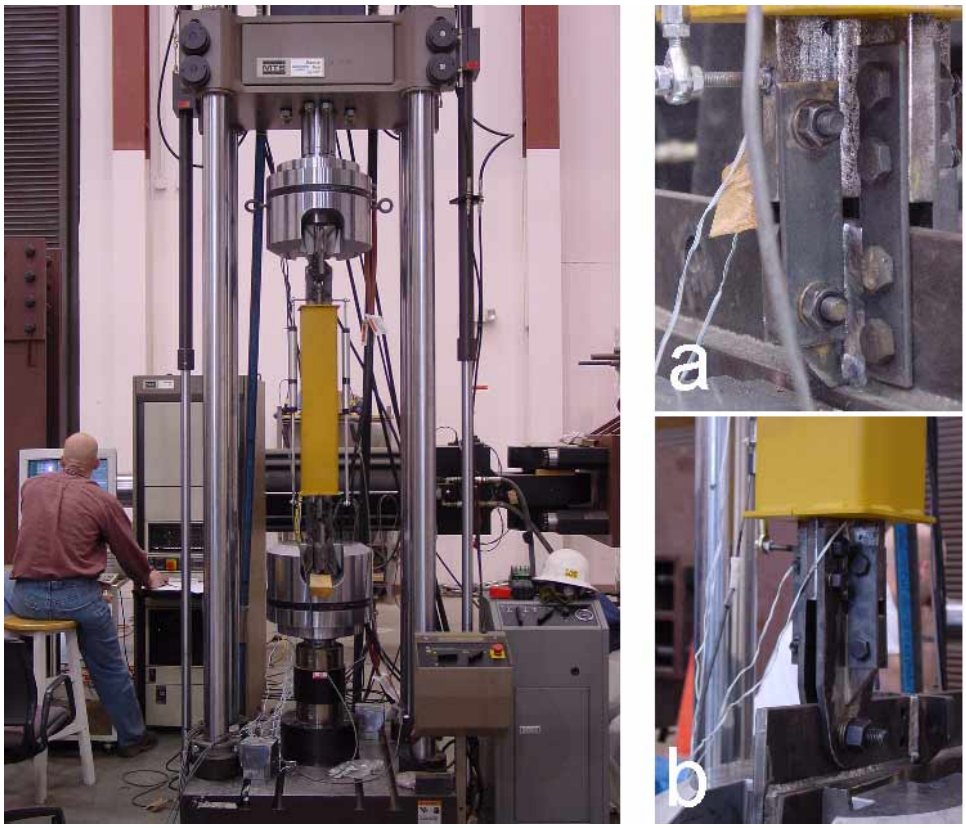

Figure 2. Experimental Setup for Axial Component Experiments on Unbonded Braces with Details a) upper right: Fixed Slip Critical Connection, and b) lower right: Pinned Connection

The remaining braces were used in experiments on the bridge model and had already been subjected to some inelastic deformation but in each case had not fractured. They were subjected to further inelastic deformation in the component experiment assembly. Unbonded Brace E was used in the north end of the bridge model. First one cycle of loading was slowly applied this brace to simulate the maximum loading in the brace during bridge experiments, then the same loading history as that applied to Brace D was applied at a dynamic rate of 2 Hz. Unbonded Brace F was the brace used in the south end of the bridge model. It was subjected to a cycle of loading equal to the maximum cycle measured during the bridge experiments then cycled to failure at a constant relatively low amplitude. The remaining brace,

Unbonded Brace G, was the brace in the midspan of the bridge model. It was subjected to one cycle as seen in the bridge model followed by a few large amplitude reversals until failure.

Hysteretic Properties

The force-displacement curves for the first four unbonded braces are shown in Figures 3-6. The hysteresis loops exhibit good energy dissipation characteristics and repeatable behavior. Figure 3 shows that there was a large difference between the displacements measured across the deformable length and the total displacement in Brace A. This was due to slippage, which was expected in the pinned ended connection. The remaining braces were designed to have slip critical connections, with slippage expected to occur, based on the AISC [11] serviceability criteria for slip critical connections, at a force of 40.1 kip. Figure 4 shows that for Brace B there was little difference between the overall displacement and displacement measured across the deformable length of the brace at low amplitude cycles. The small difference can be attributed to elastic deformations in the connection region. At the large amplitude cycles however the difference between the displacements increased, indicating some slippage, at a maximum force level of -30.6 kips. This was lower than the calculated slippage force. For Brace C no slippage was observed with a maximum force of -31.0 kips. More slippage was observed in the dynamic experiments with Braces D and E and the with the large amplitude displacements of Brace G. Therefore, although the bolts were consistently tightened with a torque wrench, the force at which slippage was expected was unconservative in these experiments, particularly when loads were applied dynamically.

A series of properties used to characterize BRBs were calculated for each brace. The yield force for each unbonded brace was estimated using the force at a 0.2% offset strain. The overstrength factor, ω, describes the maximum measured tensile force measured in the brace divided by the expected yield strength. The compression strength adjustment factor, β, is defined as the maximum compression force divided by the maximum tension force. These values are tabulated in Table 2 for each of the unbonded braces.

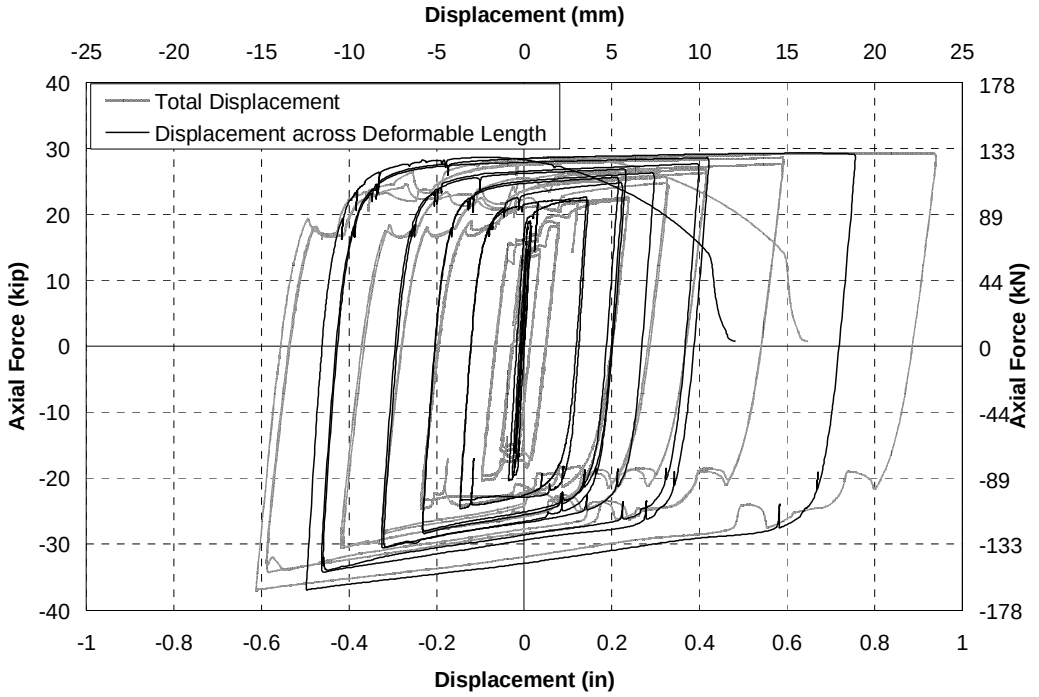

Figure 3. Hysteresis loop for Component Experiment of Unbonded Brace A – Pseudo-static Modified ATC-24 History

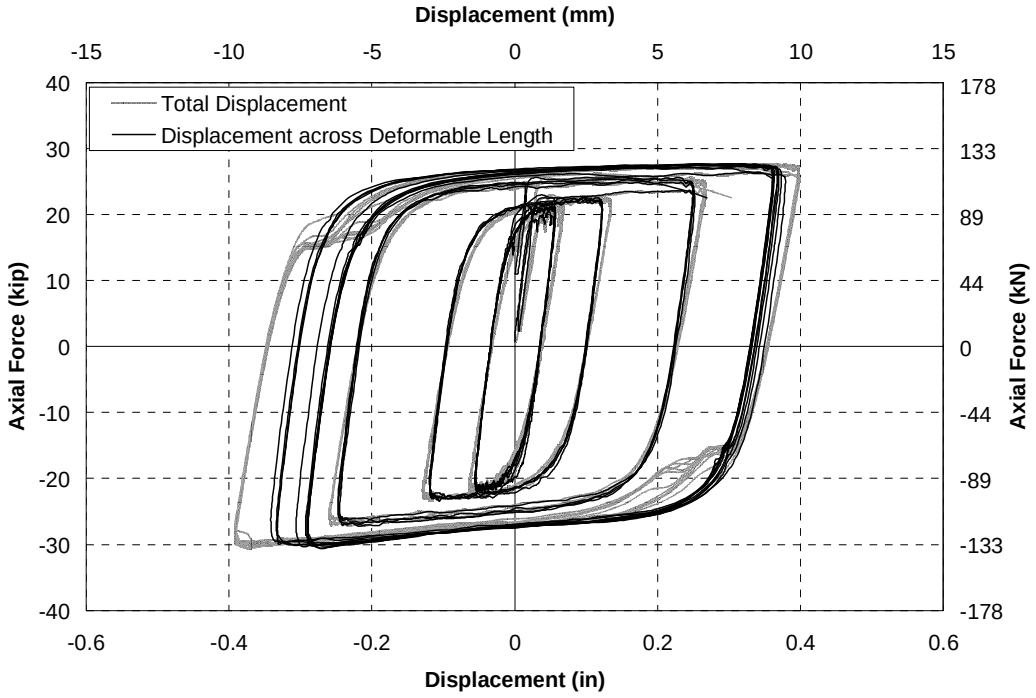

Figure 4. Hysteresis loop for Component Experiment of Unbonded Brace B– Pseudo-static BRBF History

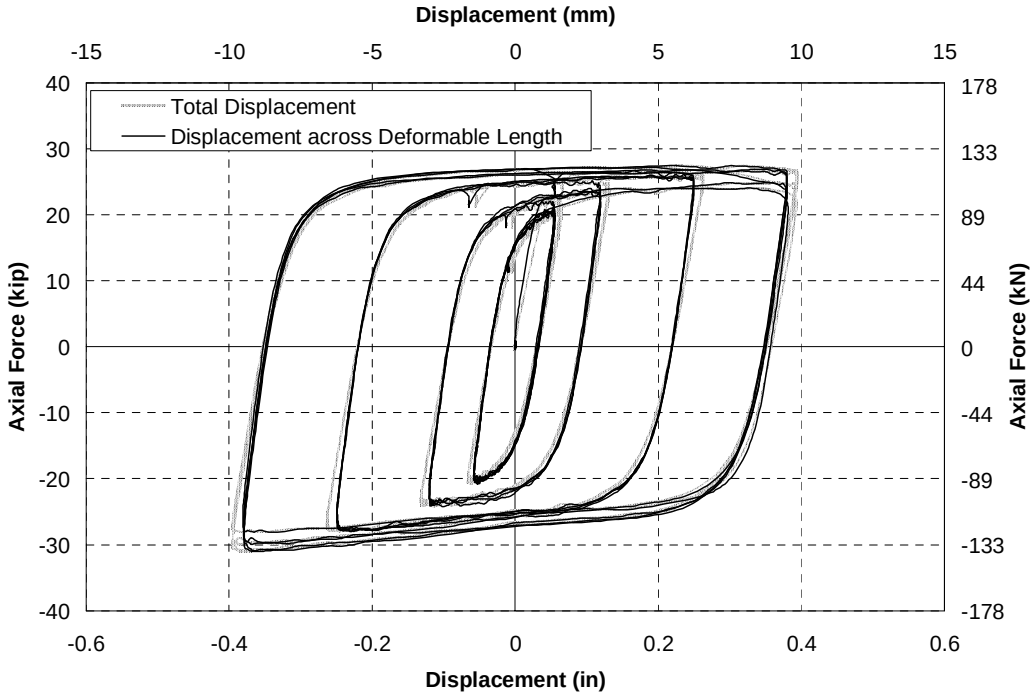

Figure 5. Hysteresis loop for Component Experiment of Unbonded Brace C – Pseudo-static Reverse BRBF History

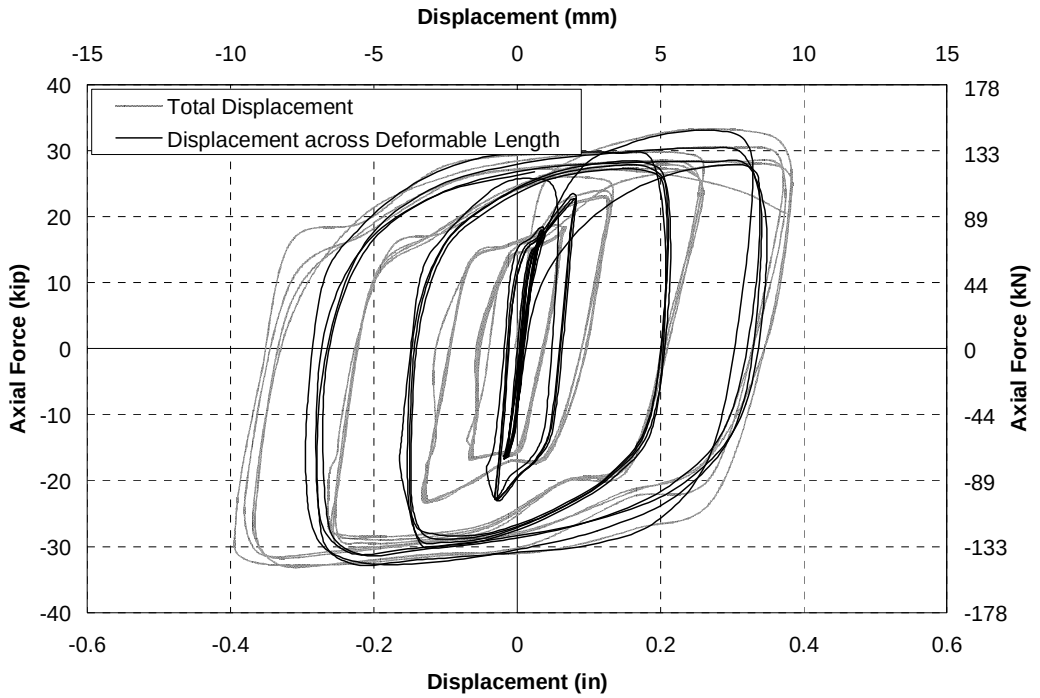

Figure 6. Hysteresis loop for Component Experiment of Unbonded Brace D – Dynamic Reverse BRBF History

Table 2. Summary of Properties for Unbonded Braces

Brace	Loading History	Expected Yield Force (kN)	Measured Yield Force (kN)	Maximum Tension Force (kN)	Maximum Compres. Force (kN)	ω	β
A	Modified ATC-24	91	96	130	-164	1.44	1.26
B	Normal Static	91	94	123	-136	1.36	1.11
C	Reversed Static	91	101	122	-138	1.35	1.13
D	Reversed Dynamic	91	102	147	-145	1.62	0.99
E	Bridge and Reversed Dynamic	91	96	140	-167	1.55	1.19
F	Bridge and Constant Static	91	96	124	-135	1.37	1.08
G	Bridge and Constant Static	91	98	134	-154	1.47	1.15

ω = maximum measured tension force divided by the expected yield force

β = ratio of maximum compression force to maximum tension force

Table 2 shows that the measured yield forces were slightly larger than the expected yield forces but within 12% in all cases. The ω factors for forces in tension were generally around 1.35 but were larger in some instances. Unbonded Brace D had the largest overstrength factor and was attributed to strain rate effects which increased the force in the brace, particularly during the first cycle of the loading. This can be observed comparing Figures 5 and 6 which compare the response to the same loading history applied slowly for Unbonded Brace C and dynamically for Brace D. In Brace D the forces in the first cycle were 30% larger than for the comparable cycle in Brace C. This 30% difference due to a higher strain rate is much larger than might be expected. As it was based on just one experiment, further study is needed. After the first cycle the difference between the braces loaded statically and dynamically reduced and stabilized to around 10 - 15%. Although not shown, Brace E had been previously loading in the bridge model and as a result the first cycle of dynamically applied loading was around 10 - 15% larger than the comparable cycle in Brace C. The braces subjected to larger maximum strains, Unbonded Braces A and G, also exhibited larger ω factors.

The compression strength adjustment factor, β, was typically around 1.10 to 1.15. β was largest for the braces with the largest maximum strains in the brace, as shown for Braces A and G, while the reverse is true for smaller strains as in Brace F. This is attributed to increased friction between the core plate and the surrounding material as the axial compression deformations increased, in part due to high mode buckling effects. For Brace D the maximum compression force was actually less than the maximum tension force due to the large observed tension force in the first reversal of the dynamically loaded specimen.

Ultimate and Cumulative Displacement Capacity

The maximum displacements, converted to equivalent strains across the deformable length of the unbonded braces during each of the component experiments, are given in Table 3. For the standard BRBF history the maximum strain was approximately 1.9% although slightly less in cases where slippage occurred. The maximum strain in Brace A was 3.7 %. These strains are consistent with levels from past experiments on unbonded braces [14].

Table 3. Cumulative Plastic Ductilities for Unbonded Braces

Brace	Loading History	Maximum Applied Strain (%)		Cumulative Plastic Ductility	
		Bridge	Component	Bridge	Component
1	Modified ATC-24	-	3.71	-	479
2	Normal Static	-	1.86	-	875
3	Reversed Static	-	1.87	-	588
4	Reversed Dynamic	-	1.71	-	337
5	Bridge and Reversed Dynamic	1.76	1.77	366	352
6	Bridge and Constant Static	2.22	0.92	205	1109
7	Bridge and Constant Static	2.29	2.51	674	192

The cumulative displacement capacity was evaluated for each brace using cumulative plastic ductility. This was calculated using an algorithm which added the displacements in excess of the calculated yield displacement after each reversal of loading. The yield displacement was assumed to be equal to the theoretical yield displacement over the deformable length using the expected yield stress for the LYP-225 material. This resulted in a yield displacement of 0.58 mm (0.0229 in). Note that this estimate of the yield displacement was around 29% less than the average yield displacement measured in the braces using the ATC-24 [12] procedure. Furthermore the calculated yield displacement was only approximately 36% of the displacement calculated at a 0.2% offset strain. The difference highlights the importance of clearly defining the method in which the yield displacement is calculated. The theoretical yield displacement was used as it was consistent between braces and with previous experiments, and also computable. The resulting calculated cumulative plastic ductilities for each specimen are given in Table 3.

Comparing the cumulative plastic ductilities and maximum strains in Braces A and B, both with increasing amplitude statically applied loading, showed that a larger maximum strain reduced the cumulative displacement capacity of the braces, as one might expect. Comparing Braces B and C, with the normal and reversed, slowly applied BRBF loading histories, showed that having the large amplitude cycles at the beginning of the history reduced the overall cumulative plastic ductility capacity of the brace. The reduction when these two braces were compared was 33%. Furthermore, applying the loading history dynamically as in Brace D further reduced the cumulative plastic capacity. Although Brace E, which was subjected to deformations in the bridge model as well as in the load frame had a similar total cumulative plastic ductility as Brace C. It was difficult to draw definitive conclusions from those braces used in the bridge model as their loading histories were highly variable. Again the range of cumulative plastic ductilities was similar to the range measured in previous experiments [14].

TRANSVERSE SEISMIC PERFORMANCE OF BRIDGE MODEL WITH UNBONDED BRACES

Braces with Pin Ended Connections

The bridge model, with unbonded braces in the ends (Figure 1), was excited with increasing amplitude motion in the transverse direction. Because the braces were relatively short compared to those typically used in building applications, flexural action in the braces was expected to be potentially significant. While the axial properties of these braces are relatively well understood, the flexural properties are not. Therefore in order to eliminate bending moments in the braces, they were designed with pinned connections to the bearing stiffeners.

The force-displacement curve for the north end of the bridge, due to the north-south component of the 1940 El Centro earthquake scaled by a factor 2.0 is shown in Figure 7. The south end, although not given, shows a similar response. The displacement was measured as the relative transverse displacement between the top and bottom flanges of the girders. The end shear was measured using load cells underneath each bearing. There was a large amount of slippage in the connections between the unbonded brace and the bearing stiffeners. At this level of excitation, and with the slippage in the connections, the inelastic deformation measured across the deformable length of the brace accounts for only a relatively small proportion of the overall deformation in the end region. Nevertheless, the overall hysteretic behavior is stable with reasonable energy dissipation despite the hysteresis loop showing a fair amount of pinching due to slippage.

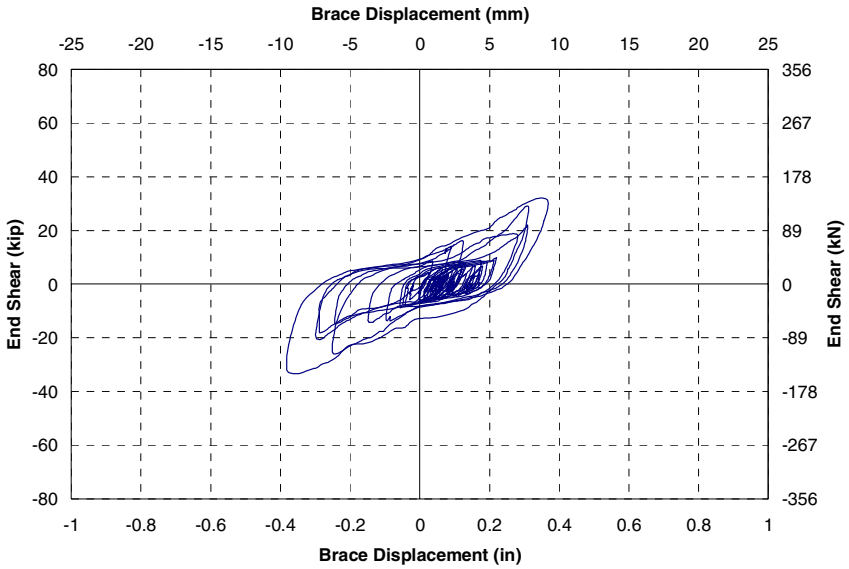

Figure 7. Hysteretic loop for Unbonded Brace with Pinned Connections at North End in Response to 2.0 x El Centro 1940

Braces with Fixed Ended Connections

Due to the large amount of slippage with the pinned connections, the connections were welded to simulate a slip critical fully fixed connection. The resulting hysteresis loop at the north end of the bridge in response to 2.0 x El Centro applied in the transverse direction is shown in Figure 8. This figure shows that the apparent stiffness had increased in the prevention of slippage and the resulting displacements had decreased. The maximum force in the system at this level of excitation increased a small amount. The displacements across the deformable length of the braces also increased, and can account for 85% of the total displacement in the end region. The remaining 15% can be accounted for by the connection regions.

Small hysteresis loops can be observed inside the large hysteresis loops. These can be seen at amplitudes where the unbonded braces remained elastic. The hysteresis loops can be attributed to the top and bottom chords, bearings and other components in the transverse load path which have some hysteretic behavior associated with them.

The disadvantage of the fully fixed connections is shown when the braces were subjected to larger amplitude ground motion. The response to a JMA ground motion in the north-south direction from the 1995 Kobe earthquake is shown in Figure 9. This figure shows that the maximum force is around 2 times the maximum force measured during component experiments. Some of this increase in force is associated with the hysteretic behavior of components in the transverse load path such as bearings, stiffeners, shear studs and top and bottom chords. However, experiments to characterize the effects of these components indicate that the force in the braces was still 50% greater in the bridge model at comparable brace strains. This additional force can be attributed to flexural action in the braces. With the pin connected braces it was expected that the force would be considerably less and the effect of slippage would become less significant in response to the large amplitude Kobe excitation. No experiment was performed with the pin connections at this level of excitation.

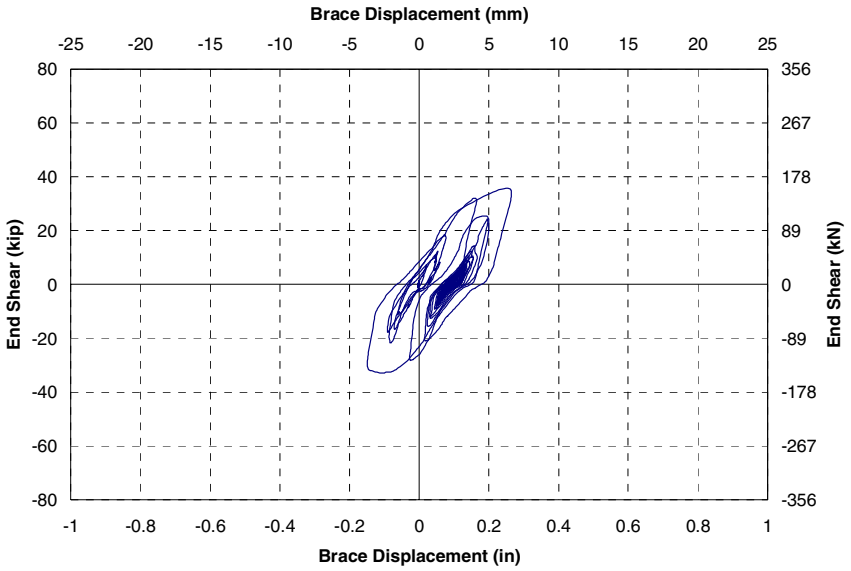

Figure 8. Hysteretic loop for Unbonded Brace with Fixed Connections at North End in Response to 2.0 x El Centro 1940

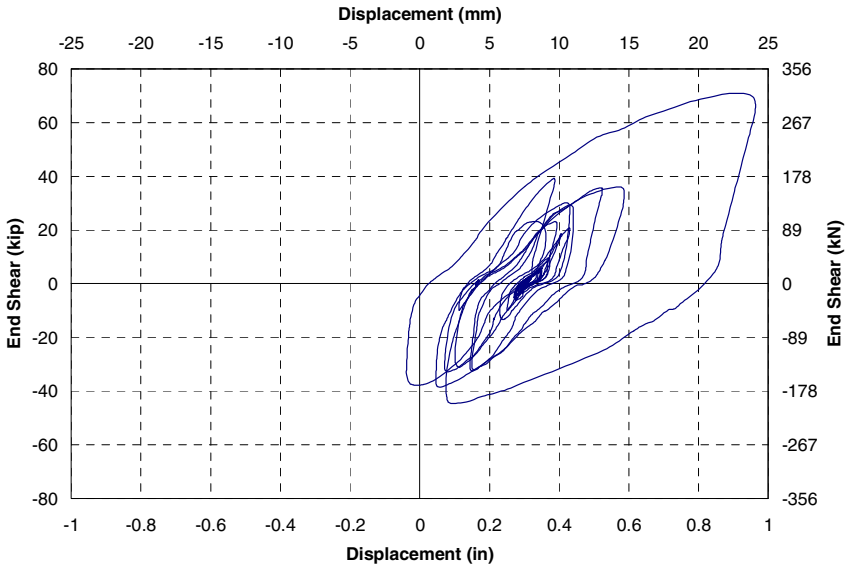

Figure 9. Hysteretic loop for Unbonded Brace with Fixed Connections at North End in Response to the north-south component recorded at the JMA station from the 1995 Kobe earthquake

It is recommended that pinned connections be used with relatively short braces required for use as ductile end cross frames to avoid uncertainty relating to flexure in the braces. In the bridge model and in component experiments no loss in performance was observed due to an increased potential for buckling in the braces using the pin ended connections compared to fixed connections. Although simple single bolt pinned connections were used in the bridge model, two bolt connections should be used as standard practice in bridge design for better high cycle fatigue performance.

COMPARISONS AND LIMITATIONS

The unbonded braces exhibited similar hysteretic behavior as previous systems used in experiments on ductile end cross frames. The maximum drift in the cross frames in response to Kobe was equal to 4%, which was larger than the ultimate drifts in the previously used ductile diaphragms which were estimated at 3.0%, 3.0% and 3.5% for SPS, EBF and TADAS systems respectively [8]. At 4% drift the braces had not failed. Based on geometry of the system, and an ultimate strain of 3.7% as measured during the component experiment on Brace A, the expected drift at failure of the brace was expected to be around 5.6%. In a full scale bridge it should be possible to increase maximum drift further with more efficient connections and a larger deformable brace length. Therefore the unbonded braces have an advantage over the other systems with a larger displacement capacity.

As well as the unbonded braces, the response of the bridge model was calculated with ductile end X-braces and elastic cross frames, up to an amplitude of 2.0 x El Centro applied in the transverse direction. The resulting maximum forces and displacements in the ends of the bridge model for the different configurations, averaged between the two ends of the bridge, in response to 2.0 x El Centro, are given in Table 3. The unbonded brace response is given for the pin ended braces. Results are normalized to the maximum force and end displacement in the bridge model with elastically responding cross frames.

Table 3. Comparisons of Bridge Model Response to 2.0 x El Centro with Different End Cross Frame Configurations

Cross Frame Configuration	Max. Shear / Elastic Shear	Max. Drift / Elastic Drift
"Heavy" X-Braces	1.00	1.00
"Light" X-Braces	0.61	7.32
Unbonded Braces	0.70	4.06

This table shows that the unbonded braces had significantly smaller displacements than the X-braces even though the forces levels were similar. Thus the unbonded braces proved to more effective than concentric X-braces even though slippage was observed in the connections.

The table also demonstrates the effect of the relatively flexible two girder bridge superstructure. The bridge model had only two girders and a relatively low transverse stiffness compared to a typical bridge with more girder lines. This meant that in order to obtain a relatively small decrease in the base shear of the structure, a relatively large increase in the end displacements was necessary. This is because the natural period of the structure was dominated not only by the effective stiffness of the cross frames but also overall stiffness of the superstructure. The same would be true if a bridge had a flexible substructure. Therefore a steel girder bridge with a superstructure that is flexurally almost rigid about its vertical axis and also has a relatively rigid substructure is likely to be the best candidate for use of ductile end cross frames. For this type of bridge the elastic period will be relatively short and the seismic demand will be at its maximum for a typical earthquake excitation. Ductile end cross frames should lengthen the period and increase damping in the structure sufficiently to allow a notable reduction in base shear. In this respect the bridge model was not the ideal bridge for the application of ductile end cross frames.

Studies were also performed on the bridge model with isolation bearings although the results are not presented here. It was possible to achieve larger displacements and therefore a larger period shift and reduction in seismic demand using seismic isolation. Therefore in general seismic isolation should also be considered as an alternative to using ductile end cross frames. However if modification of the response is only desired in the transverse direction, or there is some other reason for not using seismic isolation, then buckling restrained braces in the end cross frame are an effective system for reducing seismic demand in a steel plate girder bridge.

CONCLUSIONS AND RECOMMENDATIONS

Component experiments on a series of buckling restrained unbonded braces for use as ductile end cross frames showed that these braces had stable and repeatable ductile behavior. Loading history and strain rate reduced the cumulative plastic capacity of the braces. Dynamically applied loads resulted in larger forces than measured pseudo-statically with the difference was particularly noticeable in the first reversal.

Unbonded braces used as ductile end cross frames in a straight steel girder bridge model were able to reduce the shear demand in the bridge. While fixed ended connections had smaller displacements in the end cross frames than the pin ended connections, they resulted in considerable overstrength attributed to flexure in the braces. Pinned connections resulted in increased displacements due to slippage particularly noticeable at lower amplitude excitations, however they are recommended to prevent flexural actions in the braces. The unbonded braces resulted in much smaller displacements than corresponding X-braces. They had similar hysteretic behavior but a larger displacement capacity than the SPS, EBF and TADAS systems. The effect of a relatively flexible superstructure in the bridge model was illustrated with larger displacements than the corresponding reduction in base shear. Ductile end cross frames are believed to be most effective when both the superstructure and substructure are relatively rigid. Seismic isolation should still be considered as an alternative to using ductile end cross frames.

ACKNOWLEDGEMENTS

The authors would like to acknowledge and thank Isao Kimura and Nippon Steel Corporation for the donation of the unbonded braces towards this study. Funding for the project from CALTRANS and FHWA is gratefully appreciated.

REFERENCES

1. Astaneh-Asl A, Bolt B, McMullin KM, Donikian RR, Modjtahedi D, Cho S. “Seismic Performance of Steel Bridges during the 1994 Northridge Earthquake.” Department of Civil Engineering, University of California at Berkeley: Report UCB/CE-STEEL-94/01, 1994.
2. Bruneau M, Wilson JW, Tremblay R. “Performance of Steel Bridges during the 1995 Hyogoken-Nambu (Kobe, Japan) Earthquake.” Canadian J. of Civil Engrg. 1996; 23(3): 678-713.
3. Shinozuka M.(ed), Ballantyne D, Borcherdt R, Buckle I, O’Rourke T, Schiff A. “The Hanshin-Awaji Earthquake of January 17, 1995 Performance of Lifelines.” National Centre for Earthquake Engineering Research, Buffalo, New York: Technical Report NCEER-95-0015, 1995.
4. Carden LP, Itani AM, Buckle IG. “An Experimental Study into the Distribution of Earthquake Forces in Steel Plate Girder Bridges.” Proceedings of the Pacific Conference on Earthquake Engineering, Christchurch, New Zealand. Paper no. 60. CD Rom, February 2003.
5. Itani AM, Reno ML. “Seismic Design of Modern Steel Highway Connectors.” Proceedings of the Structure Congress XIII, Boston, MA. v2 1528-1531. ASCE, April 2-5. 1995.

6. Astaneh-Asl A. “Notes on the Cyclic Behavior and Design of Steel Bridges - Volume I - Response Modification Factor Based Design.” American Iron and Steel Institute, Washington DC: Technical Report, November, 1996.
7. Zahrai SM, Bruneau M, “Ductile End-Diaphragms for Seismic Retrofit of Slab-on-Girder Steel Bridges.” Journal of Structural Engineering 1999; 125(1): 71-80.
8. Zahrai SM, Bruneau M. “Cyclic Testing of Ductile End-Diaphragms for Slab-on-Girder Steel Bridges.” Journal of Structural Engineering 1999; 125(9): 987-996.
9. Carden, LP, Itani AM, Buckle IG. “Composite Action in Steel Girder Bridge Superstructures subjected to Transverse Earthquake Loading.” Transportation Research Record 2002; 1814: 245-252.
10. Nippon Steel Corporation. “Seismic Behavior of Typical Steel (Unbonded Brace) - Tensil Test Report for Steel Material of LYP-225.” Japan: Nippon Steel Corporation, October 2002.
11. American Institute of Steel Construction (AISC). “Manual of Steel Construction - Load Factor and Resistance Design, 2nd Edition.” Chicago, IL: AISC, 1997.
12. Applied Technology Council (ATC). “ATC 24 - Guidelines for Cyclic Seismic Testing of Components of Steel Structures.” Redwood City, CA: ATC, 1992.
13. Structural Engineering Association of Northern California (SEAoNC) BRBF ad-hoc Committee. “Recommended Provisions for Buckling-Restrained Brace Frames.” Sacramento, CA: SEAOC, July 2003.
14. Black C, Makris N, Aiken I. “Component Testing, Stability Analysis and Characterization of Buckling Restrained Unbonded Braces™.” Berkeley, CA: PEER Report 2002/08, September 2002.
15. American Association of State Highway and Transportation Officials (AASHTO). “Guide Specifications for Seismic Isolation Design, (Second Edition including Interim Revisions).” Washington, DC: AASHTO, 2000.